

Effect of surface modifications to single and multilayer graphene temperature coefficient of resistance

Jorge Torres, Yulin Liu, Seth So, Hojoon Yi, Sangho Park, Jung-Kun Lee, Seong Chu Lim, and Min Hee Yun

ACS Appl. Mater. Interfaces, **Just Accepted Manuscript** • DOI: 10.1021/acsami.0c09621 • Publication Date (Web): 28 Sep 2020

Downloaded from pubs.acs.org on October 4, 2020

Just Accepted

“Just Accepted” manuscripts have been peer-reviewed and accepted for publication. They are posted online prior to technical editing, formatting for publication and author proofing. The American Chemical Society provides “Just Accepted” as a service to the research community to expedite the dissemination of scientific material as soon as possible after acceptance. “Just Accepted” manuscripts appear in full in PDF format accompanied by an HTML abstract. “Just Accepted” manuscripts have been fully peer reviewed, but should not be considered the official version of record. They are citable by the Digital Object Identifier (DOI®). “Just Accepted” is an optional service offered to authors. Therefore, the “Just Accepted” Web site may not include all articles that will be published in the journal. After a manuscript is technically edited and formatted, it will be removed from the “Just Accepted” Web site and published as an ASAP article. Note that technical editing may introduce minor changes to the manuscript text and/or graphics which could affect content, and all legal disclaimers and ethical guidelines that apply to the journal pertain. ACS cannot be held responsible for errors or consequences arising from the use of information contained in these “Just Accepted” manuscripts.

Effect of surface modifications to single and multilayer graphene temperature coefficient of resistance

Jorge Torres¹, Yulin Liu¹, Seth So¹, Hojoon Yi², Sangho Park³, Jung-Kun Lee¹, Seong Chu Lim^{2*}, Minhee Yun^{1*}

1. Swanson School of Engineering, University of Pittsburgh, Pittsburgh, PA 15260, United States

2. Department of Energy Science and Center for Integrated Nanostructure Physics, Institute for Basic Science, Sungkyunkwan University, Suwon 440-746, Republic of Korea

3. Distributed Energy Division, Ministry of Trade, Industry & Energy, Sejong 30118, Republic of Korea

Keywords: single layer graphene, multilayer graphene, core shells, nanoparticle embedded, temperature coefficient of resistance, Ag nanoparticles

ABSTRACT: Interfacial effects on single-layer graphene (SLG) or multilayer graphene (MLG) properties greatly affect device performance. Thus, the effect of the interface on the temperature coefficient of resistance (TCR) on SLG and MLG due to surface deposited core-shell metallic nanoparticles (MNPs) and various substrates was experimentally investigated. Observed substrates included glass, SiO₂, and Si₃N₄. We show that these modifications can be used to strongly influence SLG interface effects, thus increasing TCR up to a 0.456% per K resistance change when in contact with SiO₂ substrate at the bottom surface and MNPs on the top surface. However, these surface interactions are muted in MLG due to the screening effect of non-superficial layers, only achieving a -0.0998% per K resistance change in contact with the bottom Si₃N₄ substrate and the top MNPs. We also demonstrate contrary thermal sensitivity responses between SLG and MLG after the addition of MNP to the surface.

Introduction

Graphene is a two-dimensional carbon-based material. Due to its hexagonal lattice configuration, graphene has many outstanding thermal, electrical, and optical characteristics, granting promising applications in advanced electronics. Significant efforts have been spent on studying these intrinsic properties, including multiple low temperature measurements of suspended graphene.^{1,2} While these works have greatly advanced understanding of the material itself, there is still much to learn about material surface interactions. Many of graphene's properties are due to its immense surface-area to volume ratio, however this also implies that external interfacing is a key factor in determining material behavior, and thus device performance. Different substrates and surface modifications can drastically alter graphene's most important properties, such as electrical conduction pathing.

Graphene has a theoretical electrical conductivity limit of 200,000 cm²·V⁻¹·s⁻¹, and practical experiments have observed conductivity of ~185,000 cm² V⁻¹ s⁻¹ in optimized conditions.¹ In the lattice geometry, each carbon atom covalently bonds to 3 others, leaving its 4th valence electron to form the pi and pi-star bands responsible for both dense carrier concentration and high carrier mobility. In the case of single-layer graphene (SLG), there are just two channels for carrier flow, corresponding to the top and bottom

surfaces of the layer. Ideally, these channels have an equal carrier distribution, allowing for uniform motion while under the influence of an external electric field. These electrons almost never interact with carbon, making electron-electron scattering the dominant source of carrier interactions in these channels.³

The introduction of additional layers forms multilayer graphene (MLG). The top and bottom surfaces act similarly to SLG, but every extra layer adds an interlayer channel. These interlayer channels operate under zero electric field intensity due to equal interference generated by surrounding carbon ions, leaving carriers to undergo entropic thermal motion. However, under the influence of an external electric field, the electrons in the interlayers are affected primarily by phonon and electronic scattering.³ This is significant as it creates a distinguishing property between SLG and MLG forms.

Carrier mobility's temperature dependence differs depending on whether it is flowing in a surface or interlayer channel. In SLG, the dominant electron-electron scattering is negligibly dependent on temperature and therefore suspended SLG has a very small Temperature Coefficient of Resistance (TCR). However, in MLG, the effect of temperature is much more significant as there is no electric field intensity in the interlayers. Changes in temperature strongly influence the thermal motion and the increase in temperature can actually reduce the

resistivity. This results in a negative TCR value for MLG. Additionally, since the interlayer channel has more influence in thicker graphene, the TCR is larger for isolated graphene with more layers. Thus, graphene thickness can rapidly begin to influence electrical conductivity.³

Importantly, this mobility temperature dependence can be affected by different material interfaces such as substrate and surface modification as mentioned before. The effect of adhering graphene to a substrate has been well observed to alter its conductive properties when compared to suspended graphene; however, there has been little research into specific substrate dependence. This work investigates the interface effects between three different substrates with SLG or MLG. Specifically, the TCR of graphene forms are measured when on Si₃N₄, amorphous SiO₂ (glass), and crystalline SiO₂ substrates to explore bottom channel interactions. Additionally, the effects on top channel interactions are studied by the incorporation of silver shell, silica-core metal nanoparticles (MNPs). This work aims to advance our understanding of how external influences can affect graphene conduction paths thus enabling the production of higher quality graphene devices.

Experimental Procedure

Figure 1 depicts a broad overview of the sample preparation and electric characterization process. MNPs were analyzed after full preparation, concluding with multiple TCR characterization tests.

SLG grown via CVD on copper foil was acquired commercially (Cheap Tubes Inc.). MLG was grown in-house onto precleaned copper foil (Alfa Aesar) using a standard high temperature APCVD process. After growth, the graphene/copper was spin coated with PMMA495 A₂, and backside graphene was removed by soft abrasion. The copper pieces were then cut to fit each sample and immersed in aqueous ammonium persulfate. After complete etching, graphene/PMMA was left behind. The resulting structure was transferred to a DI water bath three times for 10 minutes each time to remove contaminants before transferring onto the target substrate. The samples were dried via hot plate. The PMMA layer was then dissolved via acetone bath for 30 minutes, and the final structure was rinsed with isopropyl alcohol (IPA) and dried via hotplate.

Wet transfer of SLG and MLG samples was completed onto each of three acetone-IPA cleaned target substrates: glass, SiO₂, Si₃N₄. Once mounted, Raman spectra analysis was used to confirm and characterize quality of the MLG. The inset in Figure 1b shows the Raman spectra data (532 nm inlaser wavelength), confirming the presence and proper relation of D, G, G', and 2D peaks. Atomic force microscopy (AFM) found a thickness of ~8 nm, consistent with Raman results.

The large silver shell, silica-core nanoparticles with a diameter of 330 nm were created chemically. This size nanoparticle was chosen since it is large enough to be attached to the surface of the graphene. First, the surface of silicon oxide nanoparticle cores (300 nm in diameter)

was modified in an APTES solution (Sigma Aldrich) to prepare for shell deposition. In parallel, an HAuCl₄ solution (Sigma Aldrich) was reduced in order to form gold seeds, which were then mixed with the modified silica cores to create silica/gold seed nanoparticles. The resulting solution was mixed with AgNO₃ (Sigma Aldrich) to reduce the seed particles and grow a silver nano-shell. The shell was allowed to grow 15 nm before the process was stopped in order to ensure that the total diameter and peak absorption wavelength of MNPs was 330 nm and 800 nm, respectively. The resulting nanoparticle solution density was 10⁸ MNPs/mL. The nanoparticle surface density on each sample was then controlled to be 3E7 MNPs/cm².

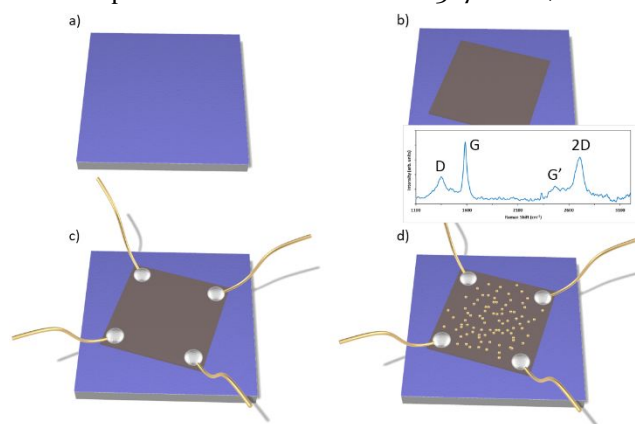


Figure 1. Overview of the sample preparation process. a) target substrate is cleaned in preparation for transfer; b) graphene transfer using a wet process. Inset: Raman spectra confirms the presence of MLG; c) contacts are soldered or wire bonded onto the graphene; d) nanoparticles are deposited onto the graphene

Sample contacts for SLG samples were made by soldering indium-tin directly onto the graphene, and MLG samples received gold contacts through wire bonding. Both sample contacts were made in the van der Pau configuration. A Hall Effect machine (Ecopia HMS-5000) was used to obtain resistivity, charge concentration, and mobility results from 310-350 K with a 10 K temperature step for SLG samples. MLG samples were tested in a vacuum cryostat from 200 K to 320 K with a 10 K temperature step. For each temperature step, 15 measurements were made and averaged together. After baseline characteristics were observed, samples were coated with the MNPs and then retested to determine how the nanoparticles on the surface of the graphene affected electrical properties of both graphene forms.

Results and Discussion

Figure 2 shows the data for SLG on glass. Figure 2a shows the sheet resistance in units of Ω/sq . Figure 2b shows the mobility in units of cm^2/Vs on the left axis and the sheet concentration in units of cm^{-2} on the right axis. The blue line with the diamond markers is the mobility while the orange line with the circle markers is the sheet concentration. All figures are shown as a function of temperature. Table 1 shows the linear fit and % change of each of these graphs. SLG on SiO₂ experiences a linear

increase in resistance as temperature increases. The mobility decreases while the sheet concentration increases over the same range. Since resistivity is inversely proportional to the mobility and the sheet concentration, this shows that the reduction in mobility is the dominant mechanism by which the resistivity increases as expected by theoretical results.³ A simple check of the % change shows that the combined change is similar to the change in resistivity. The reduction in mobility is caused by interfacial electron-phonon scattering between the graphene and the glass substrate.³ The slight increase in sheet concentration is due to increased absorption of ambient molecules.⁴

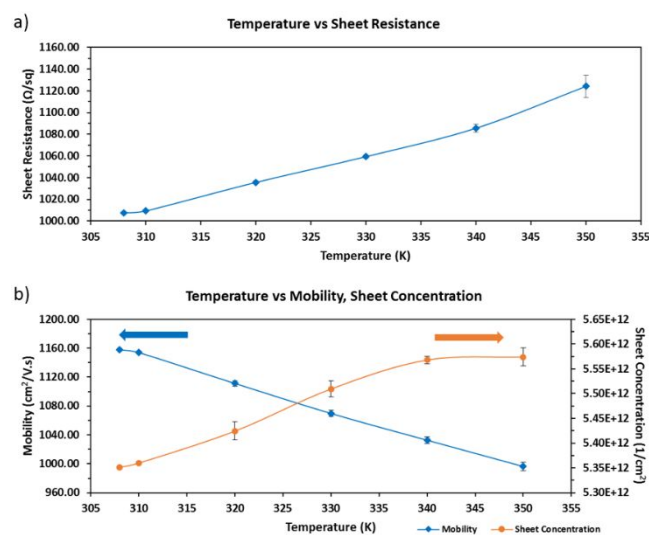


Figure 2. SLG results on glass without nanoparticles for a) Sheet Resistance, b) Mobility (blue line with diamond markers, left side axis), and Sheet Concentration (orange line with circle markers, right side axis) over the temperature range 300-350 K

Table 1. SLG on glass data in Figure 2

	Slope	310 K Value	% Change per K (310-350 K)
Sheet Resistance	2.712 $\Omega/\text{sq}/\text{K}$	1009.304 Ω/sq	0.284
Mobility	-3.914 $\text{cm}^2/\text{Vs}/\text{K}$	1150.810 cm^2/Vs	-0.341
Sheet Concentration	5.847E+09 $1/\text{cm}^2/\text{K}$	5.369E+12 $1/\text{cm}^2$	0.100

Linear fit slope, 310 K value, and % change of data shown in Figure 2 for SLG on glass

Figure 3 shows the analysis of the same SLG sample now modified with MNPs. Figure 3a shows the sheet resistance, Figure 3b shows the mobility as the blue line with the diamond markers oriented on the left axis and the sheet concentration as the orange line with circle markers oriented on the right axis. All figures are shown as a function of temperature. As before, Table 2 shows the linear fit data. Note that a linear fit for Figure 3a still shows a fit of about 90%. The MNP can be seen to cause a large

change in observed properties of graphene. The sheet resistance increases by about 100 Ω/sq as a result of the new scattering centers offered by the presence of the nanoparticles. This also causes a reduction in the magnitude of the temperature coefficient. However, this change is largely due to the swap in dominant mechanism for resistance change. Here, the mobility is increased as a result of increasing temperature and the sheet concentration decreases. Since the nanoparticles are made of a silica core surrounded by a silver shell, it is likely that the silver of the nanoparticles are causing a charge transfer to take place. The nanoparticles act as carrier absorbers and interrupt the surface channel such that increased thermal motion influences the ability of the charge carriers to flow inside the graphene.^{5,6}

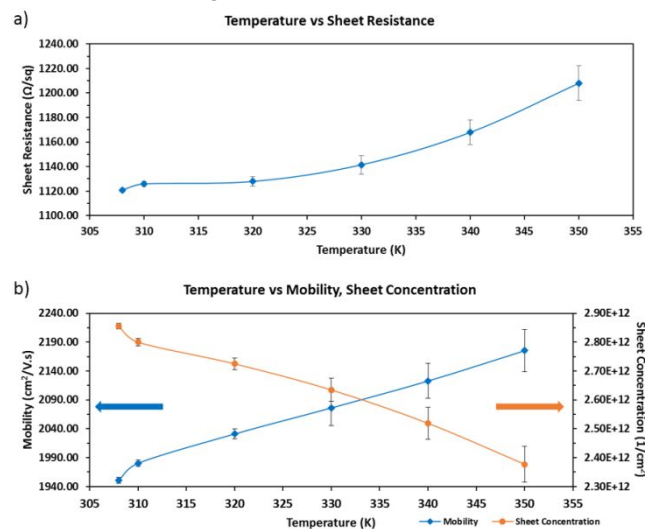


Figure 3. SLG results on glass with MNP for a) Sheet Resistance, b) Mobility (blue line with diamond markers, left side axis), and Sheet Concentration (orange line with circle markers, right side axis) over the temperature range 300-350 K

Table 2. SLG on glass with MNP data in Figure 3

	Slope	310 K Value	% Change per K (310-350 K)
Sheet Resistance	1.893 $\Omega/\text{sq}/\text{K}$	1117.715 Ω/sq	0.182
Mobility	5.082 $\text{cm}^2/\text{Vs}/\text{K}$	1972.971 cm^2/Vs	0.246
Sheet Concentration	-1.068E+10 $1/\text{cm}^2/\text{K}$	2.826E+12 $1/\text{cm}^2$	-0.377

Linear fit slope, 310 K value, and % change of data shown in Figure 3 for SLG on glass with nanoparticles

The data in Figure 4 shows the results of SLG on crystalline SiO_2 . Figure 4a shows the sheet resistance in ohms/sq. As before, a rise in the sheet resistance as temperature increases can be seen. Figure 4b shows the measured mobility and the sheet concentration. As previously, the blue line with the diamond markers is the mobility, oriented on the left axis, and the orange line with

the circle markers is the sheet concentration, oriented on the right axis. Table 3 shows the linear fit data. In comparison with the glass substrate, the mobility is much lower. This indicates that the ordered lattice of crystalline SiO_2 is likely providing a greater scattering source than the amorphous lattice of glass. It is known that Si does not affect graphene as strongly as O does.⁷ The ordered O atoms of the SiO_2 can thus be considered the scattering centers. Oxygen is also known to induce a p-type doping effect on graphene and this is seen by the increased sheet concentration measured.⁷ However, the mobility increases with increasing temperature while the sheet concentration decreases with increasing temperature. This is the opposite situation from the glass substrate. Through this combination, the overall percent change remains similar to the glass case.

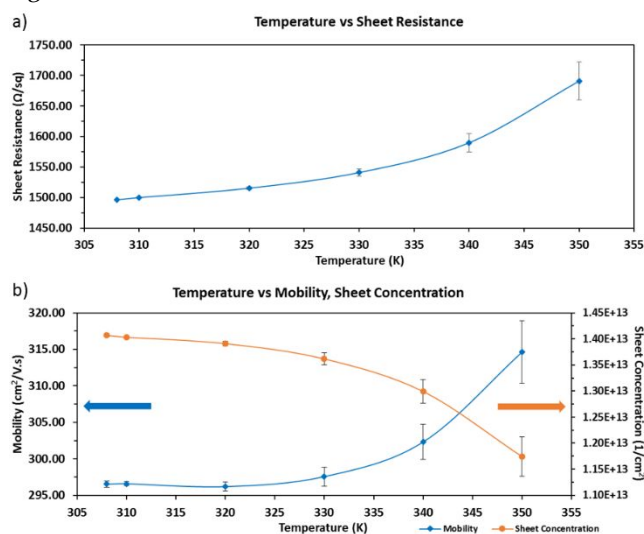


Figure 4. SLG results on SiO_2 without nanoparticles for a) Sheet Resistance, b) Mobility (blue line with diamond markers, left side axis), and Sheet Concentration (orange line with circle markers, right side axis) over the temperature range 300-350 K

Table 3. SLG on SiO_2 data in Figure 4

	Slope	310 K Value	% Change per K (310-350 K)
Sheet Resistance	4.183 $\Omega/\text{sq}/\text{K}$	1487.182 Ω/sq	0.281
Mobility	0.365 $\text{cm}^2/\text{Vs}/\text{K}$	294.671 cm^2/Vs	0.124
Sheet Concentration	-4.975E+10 $1/\text{cm}^2/\text{K}$	1.421E+13 $1/\text{cm}^2$	-0.350

Linear fit slope, 310 K value, and % change of data shown in Figure 4 for SLG on glass

Figure 5a shows the sheet resistance data for SLG on crystalline SiO_2 with MNP. As expected, the resistance value has increased due to the increased scattering centers. Additionally, there is a larger % change per K of the sheet resistance than without nanoparticles. Figure 5b shows the mobility and sheet concentration for SLG on SiO_2 with

MNP. The format follows the previous graphs. Table 4 shows the linear fit data. The mobility has seen an increase compared to without nanoparticles while the sheet concentration has decreased. The data shows similar characteristics to SLG on glass with MNP. The decrease in concentration allows for less likelihood of electron-electron scattering. This allows the mobility to increase enough to offset the decrease in carrier concentration.

The final substrate tested was Si_3N_4 . Figure 6a shows the sheet resistance of SLG on Si_3N_4 without nanoparticles. As in the other cases, the sheet resistance is increasing. Figure 6b shows the mobility and the sheet concentration, formatted as previously discussed. Table 5 shows the linear fit data. As in SiO_2 , they are increasing and decreasing respectively. Of particular interest is that SLG on Si_3N_4 has the highest resistance and most sensitivity of any of the tested substrates without nanoparticles. While some studies have indicated that Si_3N_4 has weak interactions with graphene, this was the case for β - Si_3N_4 (0001) where graphene has the potential to lie completely flat.⁸ It is unlikely that our graphene lies as flat as possible due to the wet transfer procedure. This causes an increase in resistance. Other studies indicate that our value for sheet resistance of graphene on SiN is acceptable.⁹ Since the thermal conductivity of Si_3N_4 is higher than that of SiO_2 , it is likely that the Si_3N_4 substrate helps to achieve a higher thermal response under the testing procedure. This increase in heat transfer allows the graphene to respond accordingly.

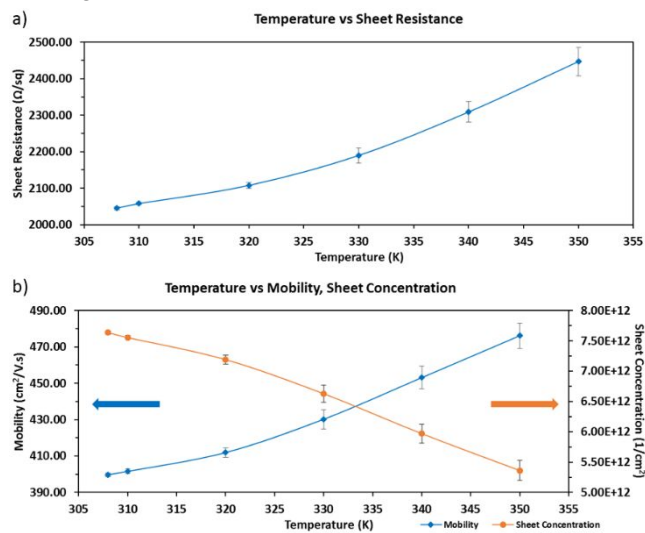


Figure 5. SLG results on SiO_2 with MNPs for a) Sheet Resistance, b) Mobility (blue line with diamond markers, left side axis), and Sheet Concentration (orange line with circle markers, right side axis) over the temperature range 300-350 K

Table 4. SLG on SiO_2 with MNP data in Figure 5

	Slope	310 K Value	% Change per K (310-350 K)
Sheet Resistance	9.297 $\Omega/\text{sq}/\text{K}$	2040.913 Ω/sq	0.456

Mobility	1.812 cm ² /Vs/K	399.203 cm ² /Vs	0.454
Sheet Concentration	-5.426E+10 1/cm ² /K	7.609E+12 1/cm ²	-0.713

Linear fit slope, 310 K value, and % change of data shown in Figure 5 for MLG on glass

The final SLG test was Si₃N₄ with MNP. Figure 7a shows the sheet resistance data gathered for this test. Figure 7b shows the mobility on the left axis using the blue line with diamond markers. Additionally, Figure 7b shows the sheet concentration on the right axis using the orange line with circle markers. Table 6 shows the linear fit data. As expected, the MNP increases the resistance as compared to without nanoparticles. However, adding MNP to SLG on Si₃N₄ results in a decrease of the % change per Kelvin of the sheet resistance. While SiN has a strong effect on the electrical channels, the temperature coupling is less significant when nanoparticles are introduced. The percent change is strongly reduced in this scenario. While the mobility slightly increases, the decrease in concentration offsets this gain and results in a weaker temperature connection. In this case, the charge transfer results in less carriers to be affected by thermal motion.^{5,6}

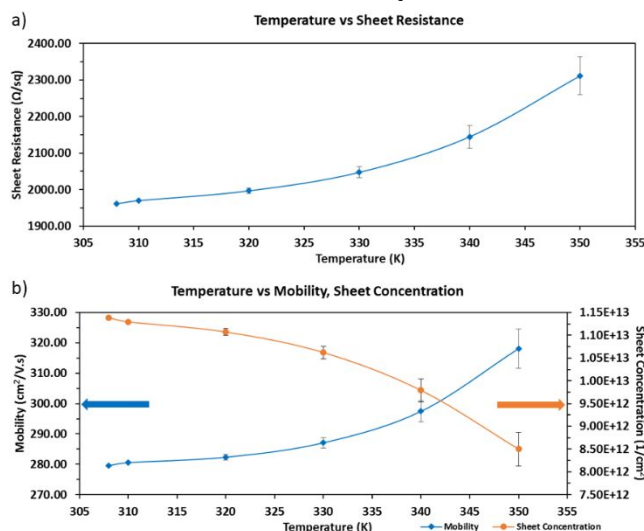


Figure 6. SLG results on SiN without nanoparticles for a) Sheet Resistance, b) Mobility (blue line with diamond markers, left side axis), and Sheet Concentration (orange line with circle markers, right side axis) over the temperature range 300-350 K

Table 5. SLG on SiN data in Figure 6

	Slope	310 K Value	% Change per K (310-350 K)
Sheet Resistance	7.659 Ω/sq/K	1946.703 Ω/sq	0.393
Mobility	0.820 cm ² /Vs/K	277.450 cm ² /Vs	0.296
Sheet Concentration	-6.373E+10 1/cm ² /K	1.149E+13 1/cm ²	-0.555

Linear fit slope, 310 K value, and % change of data shown in Figure 6 for MLG on glass

Testing was repeated with MLG equivalents of the previous samples in order to observe the effects of different substrates on the resistivity and TCR of multilayer graphene. As a direct comparison to the SLG samples, Figure 8 shows the results for MLG on glass. The blue line with diamond markers on the left axis is MLG on glass without nanoparticles. As expected from theory, the resistance of the MLG samples goes down as temperature increases.³ This is because the increase in temperature amplifies the thermally driven carrier activity. This is opposed to the SLG behavior shown above where the resistance increases with increasing temperature. Figure 8 also shows MLG with MNPs on glass using the orange line with circle markers on the right axis. Here the resistance is increased a significant amount, showing that the nanoparticles had a pronounced presence as a scattering center. Table 7 shows the linear fit data for Figure 8. The % change per K of the sheet resistance is smaller than in the SLG case, as the substrate effect is lessened with increasing thickness of graphene. While the resistance is lower than the SLG case, this is likely due to a difference in testing protocol between SLG and MLG samples. SLG samples were tested in ambient and thus were contaminated by atmospheric particles. MLG samples were tested in vacuum and not subject to such external scattering sources. As SLG and MLG are both semimetals, ohmic contact can be assured allowing for a small contact resistance. Additionally, as both sample types were tested in the van der Pau geometry, the relatively low contact resistance can be ignored. Therefore, the difference in contacts is not problematic.

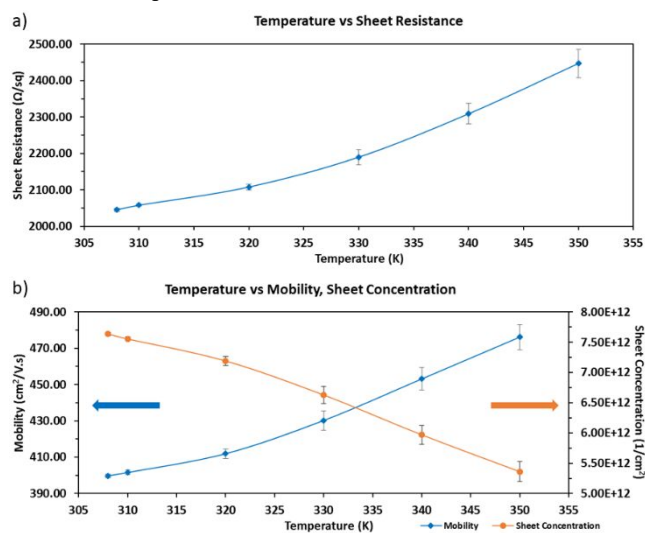


Figure 7. SLG results on SiN with MNP for a) Sheet Resistance, b) Mobility (blue line with diamond markers, left side axis), and Sheet Concentration (orange line with circle markers, right side axis) over the temperature range 300-350 K

Table 6. SLG on SiN with MNP data in Figure 7

	Slope	310 K Value	% Change per K (310-350 K)
Sheet Resistance	7.659 Ω/sq/K	1946.703 Ω/sq	0.393
Mobility	0.820 cm ² /Vs/K	277.450 cm ² /Vs	0.296
Sheet Concentration	-6.373E+10 1/cm ² /K	1.149E+13 1/cm ²	-0.555

Sheet Resistance	2.238 $\Omega/\text{sq}/\text{K}$	2349.740 Ω/sq	0.095
Mobility	0.826 $\text{cm}^2/\text{Vs}/\text{K}$	325.342 cm^2/Vs	0.254
Sheet Concentration	-2.533E+10 $1/\text{cm}^2/\text{K}$	8.152E+12 $1/\text{cm}^2$	-0.311

Linear fit slope, 310 K value, and % change of data shown in Figure 7 for MLG on glass

Figure 9 shows MLG on a crystalline SiO_2 substrate using the blue line with diamond markers oriented along the left axis. The orange line with circle markers oriented along the right axis in Figure 9 shows MLG with MNPs on a crystalline SiO_2 substrate. Unlike the amorphous glass case, the presence of ordered SiO_2 increases the interfacial scattering between the graphene and the substrate layers. This interfacial scattering decreases the magnitude of the % change per Kelvin of the sheet resistance as the electron-phonon scattering present reduces the mobility in the bottom most layers of graphene.³ The linear fit data in Table 8 show this change. As it is known that the O atoms in SiO_2 are mainly responsible for the scattering effect on graphene, it is likely that the ordered SiO_2 results in more opportunities for the O atom to interact with graphene than in the unordered case of glass.⁷

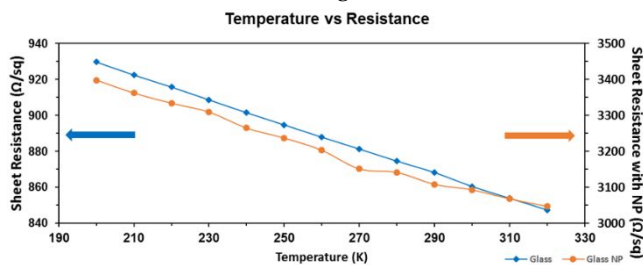


Figure 8. Sheet resistance of MLG on glass with no nanoparticles (blue line, diamond markers, left side axis) and MNP (orange line, circle markers, right side axis)

Table 7. MLG on glass data in Figure 8

	Slope ($\Omega/\text{sq}/\text{K}$)	300 K Value (Ω/sq)	% Change per K (200-310 K)
Glass	-0.685	860.833	-0.0737
Glass (MNP)	-3.010	3088.748	-0.0861

Linear fit slope, 310 K value, and % change of data shown in Figure 8 for MLG on glass

The last case observed was MLG on Si_3N_4 . Figure 10 shows the results as a function of temperature. Table 9 shows the linear fit data. As is easily viewed from the graph, graphene on silicon nitride results in the lowest resistance of the three interfaces. This corresponds with experimental data from Benyamin Davaji et al.¹⁰ and is due to the reduced influence of N atoms on interfacial scattering.⁸ In this case, the addition of MNPs did not increase the measured resistance by a significant margin. Whereas the resistance increased by at least $100\Omega/\text{sq}$ in all previous cases, the resistance only shifted upwards by $30\text{-}40\Omega/\text{sq}$ in

this case. However, this MLG on Si_3N_4 with MNP sample yielded the strongest dependence on temperature as shown in Table 9. It is likely that the reduced effect on the electric field from the graphene/substrate interface within the interlayers of the MLG allow for the thermal motion of the carriers to be more prominent.

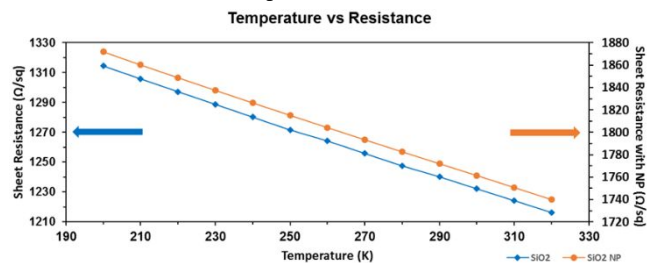


Figure 9. Sheet resistance of multilayer graphene on SiO_2 with no nanoparticles (blue line, diamond markers, left side axis) and MNP (orange line, circle markers, right side axis)

Table 8. MLG on SiO_2 data in Figure 9

	Slope ($\Omega/\text{sq}/\text{K}$)	300 K Value (Ω/sq)	% Change per K (200-310 K)
SiO_2	-0.815	1231.879	-0.0622
SiO_2 with MNP	-1.096	1761.078	-0.0587

Linear fit slope, 310 K value, and % change of data shown in Figure 9 for MLG on SiO_2

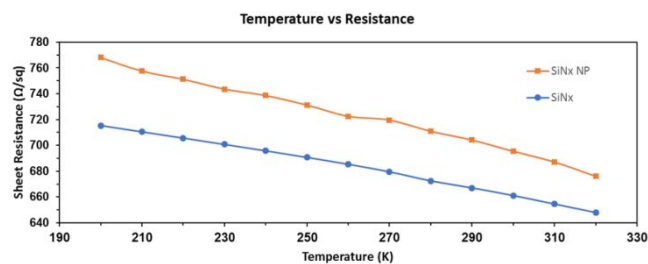


Figure 10. Sheet resistance of multilayer graphene on Si_3N_4 with MNP (orange line, square markers) and without MNP (blue line, circle markers).

Table 9. MLG on Si_3N_4 data in Figure 10

	Slope ($\Omega/\text{sq}/\text{K}$)	300 K Value (Ω/sq)	% Change per K (200-310 K)
Si_3N_4	-0.561	661.163	-0.0785
Si_3N_4 (MNP)	-0.721	694.652	-0.0998

Linear fit slope, 310 K value, and % change of data shown in Figure 10 for MLG on Si_3N_4

Conclusion

Substrate-induced scattering changes the TCR of SLG by breaking the charge symmetry of top and bottom surfaces, as well as by introducing an additional scattering source. The oxide layer of the SiO_2 acted as such a scattering source when interacting with SLG, similar to Si_3N_4 substrate. In these cases, increasing temperature increased mobility while decreasing the sheet concentration.

Without the introduction of MNPs, Si₃N₄ was found to affect the sheet resistance of the graphene the most, achieving a 0.393% change per K. With MNP, crystalline SiO₂ to provide the largest overall sheet resistance change of 0.456% per K. In the case of MLG, the effect of the substrate is screened by the bottom layer and is largely influenced by graphene thickness.¹¹ This is due to the bottom surface carriers providing a counter electric field, and the force still diminishes with distance at this scale. Therefore, substrates should have a minor interfacial scattering effect on MLG compared to SLG, which was confirmed in the data.

Top surface channel modulation was also explored in this work with the introduction of MNP. In all cases, MNP samples had higher resistance for two reasons: (1) strong surface binding caused structural deformations that are known to increase graphene's resistivity;¹² (2) the MNPs create charge transfer wells, reducing graphene carrier efficiency. This consequently affects the temperature response of the resistivity, differentiating SLG and MLG. The former exhibits a decrease in the magnitude of TCR due to decreases in efficiency. The latter displays an increase in the magnitude TCR as the effect is screened and unable to outweigh the increased thermal motion. The situation is reversed in crystalline SiO₂, likely due to the ordered influence of oxygen.

These interfacial effects play a significant, complex role in determining graphene behavior. Continued characterization of material interactions is crucial, as a better understanding will lead to improvements in quality and reliability of future graphene-based devices.

AUTHOR INFORMATION

Corresponding Author

Minhee Yun - Swanson School of Engineering, University of Pittsburgh, Pittsburgh, PA 15260, United States; Email:

miy16@pitt.edu

Seong Chu Lim - Department of Energy Science and Center for Integrated Nanostructure Physics, Institute for Basic Science, Sungkyunkwan University, Suwon 440-746, Republic of Korea

seonglim@skku.edu

Authors

Jorge Torres - Swanson School of Engineering, University of Pittsburgh, Pittsburgh, PA 15260, United States

Yulin Liu - Swanson School of Engineering, University of Pittsburgh, Pittsburgh, PA 15260, United States

Seth So - Swanson School of Engineering, University of Pittsburgh, Pittsburgh, PA 15260, United States

Hojoon Yi - Department of Energy Science and Center for Integrated Nanostructure Physics, Institute for Basic Science, Sungkyunkwan University, Suwon 440-746, Republic of Korea

Sangho Park - Distributed Energy Division, Ministry of Trade, Industry & Energy, Sejong 30118, Republic of Korea

Jung-Kun Lee - Swanson School of Engineering, University of Pittsburgh, Pittsburgh, PA 15260, United States

Author Contributions

J.T. conducted sample preparation, measurements for SLG data, analysis, and prepared the manuscript. Y.L. prepared the nanoparticles. H.Y. performed electrical measurements for MLG data. S.S. reviewed data and edited the manuscript. All authors have given approval to the final version of the manuscript.

ACKNOWLEDGMENT

Authors J.T., Y.L., S.S., J. L. and M.Y. were funded by the National Science Foundation (NSF 1709307). Authors S. L. and M. Y. were funded by the Brain Pool Program (2019H1D3A2A01060326) through the National Research Foundation of Korea (NRF).

ABBREVIATIONS

SLG, single layer graphene; MLG, multilayer graphene; TCR, Temperature Coefficient of Resistance; MNP, metal nanoparticle; CVD, chemical vapor deposition; IPA, isopropyl alcohol; AFM, atomic force microscopy.

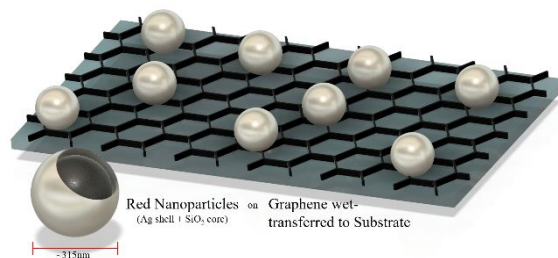
REFERENCES

- (1) Du, X., Skachko, I., Barker, A., & Andrei, E. Y. Approaching Ballistic Transport in Suspended Graphene. *Nat Nanotechnol*, vol. 3, no. 8, 20 July 2008, pp. 491–495., doi:10.1038/nnano.2008.199.
- (2) Bolotin, K. I., Sikes, K. J., Hone, J., Stormer, H. L., & Kim, P. Temperature-Dependent Transport in Suspended Graphene. *Phys. Rev. Lett.*, vol. 101, no. 9, 25 Aug. 2008, pp. 096802., doi: 10.1103/PhysRevLett.101.096802.
- (3) Fang, X. Y., Yu, X. X., Zheng, H. M., Jin, H. B., Wang, L., & Cao, M. S. Temperature- and Thickness-Dependent Electrical Conductivity of Few-Layer Graphene and Graphene Nanosheets. *Phys. Lett. A*, vol. 379, no. 37, 30 June 2015, pp. 2245–2251., doi:10.1016/j.physleta.2015.06.063.
- (4) Ryu, S., Liu, L., Berciaud, S., Yu, Y.J., Liu, H., Kim, P., Flynn, G.W., & Brus, L.E. Atmospheric Oxygen Binding and Hole Doping in Deformed Graphene on a SiO₂ Substrate. *Nano Lett.*, vol. 10, no. 12, 11 Nov. 2010, pp. 4944–4951., doi:10.1021/nl1029607.
- (5) Subrahmanyam, K. S., Manna, A. K., Pati, S. K., & Rao, C. N. R. A Study of Graphene Decorated with Metal Nanoparticles. *Chem. Phys. Lett.*, vol. 497, no. 1–3, 28 July 2010, pp. 70–75., doi:10.1016/j.cplett.2010.07.091.
- (6) Das, B., Choudhury, B., Gomathi, A., Manna, A. K., Pati, S. K., & Rao, C. N. R. Interaction of Inorganic Nanoparticles with Graphene. *ChemPhysChem*, vol. 12, no. 5, 7 Mar. 2011, pp. 937–943., doi:10.1002/cphc.201001090.
- (7) Kang, Y. J., Kang, J., & Chang, K. J. Electronic Structure of Graphene and Doping Effect on SiO₂. *Phys. Rev. B*, vol. 78, no. 11, 4 Sept. 2008, p. 115404., doi:10.1103/physrevb.78.115404.
- (8) Yang, M., Zhang, C., Wang, S., Feng, Y., & Ariando. Graphene on β-Si₃N₄: An Ideal System for Graphene-Based Electronics. *AIP Adv.*, vol. 1, no. 3, 27 July 2011, p. 032111., doi:10.1063/1.3623567.
- (9) Sun, J., Lindvall, N., Cole, M. T., Teo, K. B., & Yurgens, A. Large-Area Uniform Graphene-like Thin Films Grown by Chemical Vapor Deposition Directly on Silicon Nitride. *Appl. Phys. Lett.*, vol. 98, no. 25, 20 June 2011, p. 252107., doi:10.1063/1.3602921.
- (10) Davaji, B., Cho, H. D., Malakoutian, M., Lee, J. K., Panin, G., Kang, T. W., & Lee, C. H. A Patterned Single Layer Graphene Resistance Temperature Sensor. *Sci. Rep.*, vol. 7, no. 1, 18 Aug. 2017, p. 8811., doi:10.1038/s41598-017-08967-y.
- (11) Varchon, F., Feng, R., Hass, J., Li, X., Nguyen, B.N., Naud, C., Mallet, P., Veuille, J.Y., Berger, C., Conrad, E.H. & Magaud, L. Electronic Structure of Epitaxial Graphene Layers on SiC: Effect of

1 the Substrate. *Phys. Rev. Lett.*, vol. 99, no. 12, 20 Sept. 2007, p.
2 126805., doi:10.1103/physrevlett.99.126805.

3 (12) Lee, J.K., Yamazaki, S., Yun, H., Park, J., Kennedy, G.P.,
4 Kim, G.T., Pietzsch, O., Wiesendanger, R., Lee, S., Hong, S. &

5 Dettlaff-Weglikowska, U. Modification of Electrical Properties of
6 Graphene by Substrate-Induced Nanomodulation. *Nano Lett.*, vol.
7 13, no. 8, 12 July 2013, pp. 3494–3500., doi:10.1021/nl400827p.



For Table of Contents Only

1
2
3
4
5
6
7
8
9
10
11
12
13
14
15
16
17
18
19
20
21
22
23
24
25
26
27
28
29
30
31
32
33
34
35
36
37
38
39
40
41
42
43
44
45
46
47
48
49
50
51
52
53
54
55
56
57
58
59
60